The Journal of Neuroscience, December 15, 1998, *18*(24):10709–10723

Rhythmic Properties of the Hamster Suprachiasmatic Nucleus *In Vivo*

Shin Yamazaki, Marie C. Kerbeshian, Craig G. Hocker, Gene D. Block, and Michael Menaker

National Science Foundation Center for Biological Timing, Department of Biology, University of Virginia, Charlottesville, Virginia 22903

We recorded multiple unit neural activity [multiunit activity (MUA)] from inside and outside of the suprachiasmatic nucleus (SCN) in freely moving male golden hamsters housed in running-wheel cages under both light/dark cycles and constant darkness. The circadian period of MUA in the SCN matched the period of locomotor activity; it was ~24 hr in wild-type and 20 hr in homozygous *tau* mutant hamsters. The peak of MUA in the SCN always occurred in the middle of the day or, in constant darkness, the subjective day. There were circadian rhythms of MUA outside of the SCN in the ventrolateral thalamic nucleus, the caudate putamen, the accumbens nucleus, the medial septum, the lateral septum, the ventromedial hypothalamic nucleus, the medial preoptic region, and the stria medullaris. These rhythms were out-of-phase with the electrical rhythm in the SCN but in-phase with the rhythm of locomotor activity, peaking during the night or subjective night. In addition to circadian rhythms, there were significant ultradian rhythms present; one, with a period of ~80 min, was in antiphase between the SCN and other brain areas, and another, with a period of ~14 min, was in-phase between the SCN and other brain areas. The periods of these ultradian rhythms were not significantly different in wild-type and *tau* mutant hamsters. Of particular interest was the unique phase relationship between the MUA of the bed nucleus of the stria terminalis (BNST) and the SCN; in these two areas both circadian and ultradian components were always in-phase. This suggests that the BNST is strongly coupled to the SCN and may be one of its major output pathways. In addition to circadian and ultradian rhythms of MUA, neural activity both within and outside the SCN was acutely affected by locomotor activity. Whenever a hamster ran on its wheel, MUA in the SCN and the BNST was suppressed, and MUA in other areas was enhanced.

Key words: circadian; ultradian; suprachiasmatic nucleus; in vivo *recording; hamster;* tau *mutant; locomotor activity; bed nucleus of the stria terminalis; MUA*

Circadian locomotor activity rhythms in mammals are generated by an endogenous pacemaker located in the suprachiasmatic nucleus (SCN) of the hypothalamus (for review, see Turek, 1985; Meijer and Rietveld, 1989; Klein et al., 1991). Lesions of the SCN cause arrhythmicity of locomotor activity (Moore and Eichler, 1972; Stephan and Zucker, 1972; Rusak and Zucker, 1979), and transplants of fetal SCN tissue restore circadian periodicities (Sawaki et al., 1984; Lehman et al., 1987; Ralph et al., 1990). The SCN exhibits circadian rhythms in several *in vitro* preparations: the acute slice (Green and Gillette, 1982; Groos and Hendricks, 1982; Shibata and Moore, 1988), slice culture (Bos and Mirmiran, 1990; Herzog et al., 1997), and dispersed cell culture (Welsh et al., 1995; Liu et al., 1997). Both slice and dispersed cell cultures of SCN also display circadian rhythms of peptide release (Murakami et al., 1991; Watanabe et al., 1993; Shinohara et al., 1995). In contrast the physiology of the SCN *in vivo* and its relationship to circadian behavior in the intact animal have received little experimental attention.

To understand how the circadian clock controls locomotor behavior, we need to understand its connections to the motor control system. Although output pathways from the SCN circadian pacemaker are not completely described, the motor control system in mammals is relatively well characterized (Wichmann et al., 1995; Bergman et al., 1998). Because there are no known direct neural connections between the SCN and motor control areas of the brain, it is likely that either humoral factors and/or "relay nuclei" serve to connect the SCN with the motor centers.

Not only does the SCN regulate locomotor activity but there is reason to believe that locomotor activity feeds back on the SCN. The period of the free-running rhythm of rats housed in cages with a running wheel is different from that of rats housed in cages without a wheel (Yamada et al., 1988, 1990; Shioiri et al., 1990). Locking of the running wheel changes the free-running period in mice (Edgar et al., 1991). Access to running wheels induces phase shifts of locomotor activity in hamsters (Mrosovsky, 1988; Reebs and Mrosovsky, 1989) as does injection of triazolam, which increases locomotor activity (van Reeth et al., 1987). In mice, forced treadmill running induces phase shifts of circadian rhythms and is able to entrain them (Marchant and Mistlberger, 1996).

The apparent complexity of the relationship between the SCN and locomotor centers, almost certainly involving reciprocal in-

Received July 29, 1998; revised Sept. 28, 1998; accepted Oct. 1, 1998.

This research was supported by the National Science Foundation (NSF) Science and Technology Center for Biological Timing along with Air Force Grants F49620-98-1-0174 to M.M. and F49620-97-1-0012 to G.D.B and M.M., by the National Institutes of Health postdoctoral National Research Service Award NS09329 to C.G.H., and by an NSF postdoctoral fellowship in Biosciences Related to the Environment to M.C.K. We thank Dr. M. E. Geusz for computer programming for recording neural activity (for spike discrimination) and Dr. M. Kawasaki for discussing amplifier circuit design. Also our special thanks to Drs. M. Takahashi and M. Nishihara for general information on multiunit activity recording and to Dr. S.-I. T. Inouye for information on electrode design.

We dedicate this work to Professor Hiroshi Kawamura on the occasion of his 70th birthday (January 26, 1997).

Correspondence should be addressed to Dr. Shin Yamazaki, National Science Foundation Center for Biological Timing, Department of Biology, Gilmer Hall, University of Virginia, Charlottesville, VA 22903.

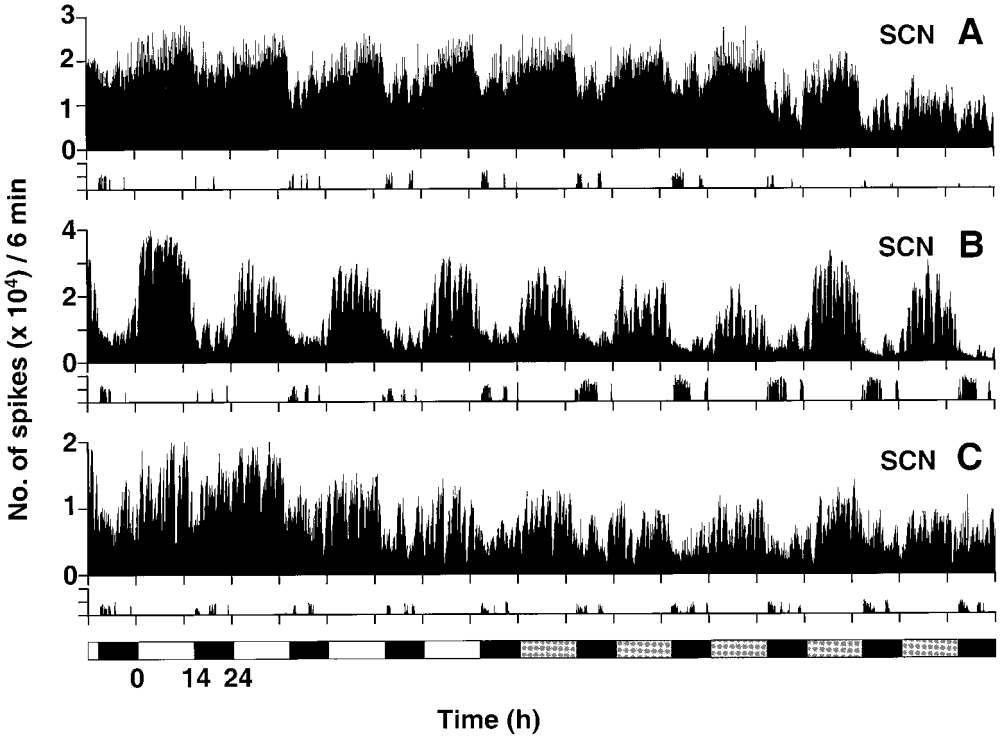

Figure 1. Examples of MUA recorded for 10 d from the SCN of three wild-type hamsters. Animals were kept in light/dark cycles (14:10 hr LD) for 4 d and then released into constant darkness (lighting condition indicated at the *bottom* of the figure). Neuronal spikes are plotted in 6 min bins. Wheel-running activity is plotted at the *bottom* of *A–C* as the number of revolutions per 6 min; the *y*-axis for this portion of the figure shows 0–200 revolutions per 6 min. *A*, Recorded from the ventrolateral portion of the central region of the left SCN. *B*, Recorded from the ventromedial portion of the right SCN at the center of the rostrocaudal axis. *C*, Recorded from the ventromedial portion of the right SCN near the caudal end of the nucleus.

teractions, and the fact that direct neuronal interconnections appear to be absent provide a strong rationale for exploring the functional relationships *in vivo*. We have perfected a technique that allows us to record neuronal activity of several brain regions in freely moving hamsters, enabling us to correlate electrical activity within the SCN with activity in other brain regions and with locomotor activity. We have used this technique to describe the electrical characteristics of the SCN *in vivo*, the differences between the *tau* mutant and wild-type hamsters, the relationship between the SCN and other regions of the brain, and the effect of the animal's locomotor behavior on SCN activity. The results provide a new framework for understanding the regulation of locomotor behavior by the circadian timing system.

MATERIALS AND METHODS

Animals. Three- to five-month-old golden hamsters (LVG wild type from Charles River Laboratories, Wilmington, MA; LVG background *tau* mutant animals from our colony) were used in this study. Animals were entrained for at least 2 weeks to light/dark cycles (LDs) (14:10 hr LD for wild types; 11.7:8.3 hr LD for *tau* mutants; light intensity of ~300 lux at cage level). We monitored wheel-running activity throughout the experiments and used only animals that showed clear locomotor rhythmicity.

Electrode implantation. We implanted one or two bipolar electrodes constructed from pairs of Teflon-coated stainless steel wires (bare diameter, 130 μm; A-M Systems, Everett, WA; tip distance, ~150 μm for recording from the SCN and 200–300 μm for other brain regions) and an uncoated platinum–iridium wire (diameter, 130 μm; A-M Systems) used as a signal ground in the cortex. Wires were connected to an eight pin IC socket wrapped in insulated copper tape. Distances between any two bipolar electrodes were determined according to the recording sites chosen.

Electrode implantation was performed under pentobarbital anesthesia (90 mg/kg, i.p.). Animals were placed in a stereotaxic instrument with the nose bar set at −2 mm (David Kopf Instruments, Tujunga, CA). Four self-tapping screws (#0 × 1/8 inch; Small Parts, Miami Lakes, FL) were implanted into 1 mm holes in the skull made with a dental drill. We used different stereotaxic coordinates for wild-type and *tau* mutant hamsters because the shape of bregma in *tau* mutants is different and more variable than is that in wild types. Wild-type SCN coordinates were 0.7 mm anterior to bregma, 0.2 mm lateral to the midsagittal, and 8.0–8.2 mm below the dural surface. *Tau* mutant coordinates were 1.0–1.2 mm anterior to bregma, 0.2 mm lateral to the midsagittal, and 7.9–8.1 mm below the dural surface. The electrode was secured to the screws and the skull with dental cement.

Recording procedure. One week after surgery, each hamster was transferred to a 24 cm (width) × 21 cm (length) × 30 cm (height) cage with a running wheel 21 cm in diameter mounted on one side to allow the hamster equipped with wires access to the wheel. The electrodes were connected to head stage buffer amplifiers (J-FET input OP Amp; TL084) located on the hamster's head. Buffer amplifiers were connected to a 12 channel slip ring (Airflyte Electronics Company, Bayonne, NJ) that allowed free movement for the animal. The wires between the head stage amplifiers and the slip ring were protected by a stainless steel spring. Output signals were processed by differential input integration amplifiers (INA 101 AM; Burr-Brown, Tucson, AZ; gain, ×10) and then fed into AC amplifiers (OP Amp, 4558; bandpass, 500 Hz to 5 kHz; gain, 10,000). Spikes were discriminated by amplitude and counted in 1 min bins using a computer-based window discrimination system (DAS-1801ST AD board; Keithley Metrabyte, Taunton, MA). Wheel revolutions were recorded using the Data Quest system (Data Science International, St. Paul, MN).

Reduction of recording noise. In recording neural activity from freely moving animals, the biggest problem is noise. We reduced microphonic noise, which is caused by mechanical disturbances such as wire movements, by mounting the buffer amplifiers on the head (effectively decreasing the impedance). We directly coupled the output signals to the integration amplifier (without any capacitors or resistors) to provide a high common mode rejection ratio that can reduce non-neuronal signals such as muscle potentials. We also used shielding material around the electrode and its vicinity to reduce noise from the animal's scratching. Because we could not entirely remove this source of noise, we used a

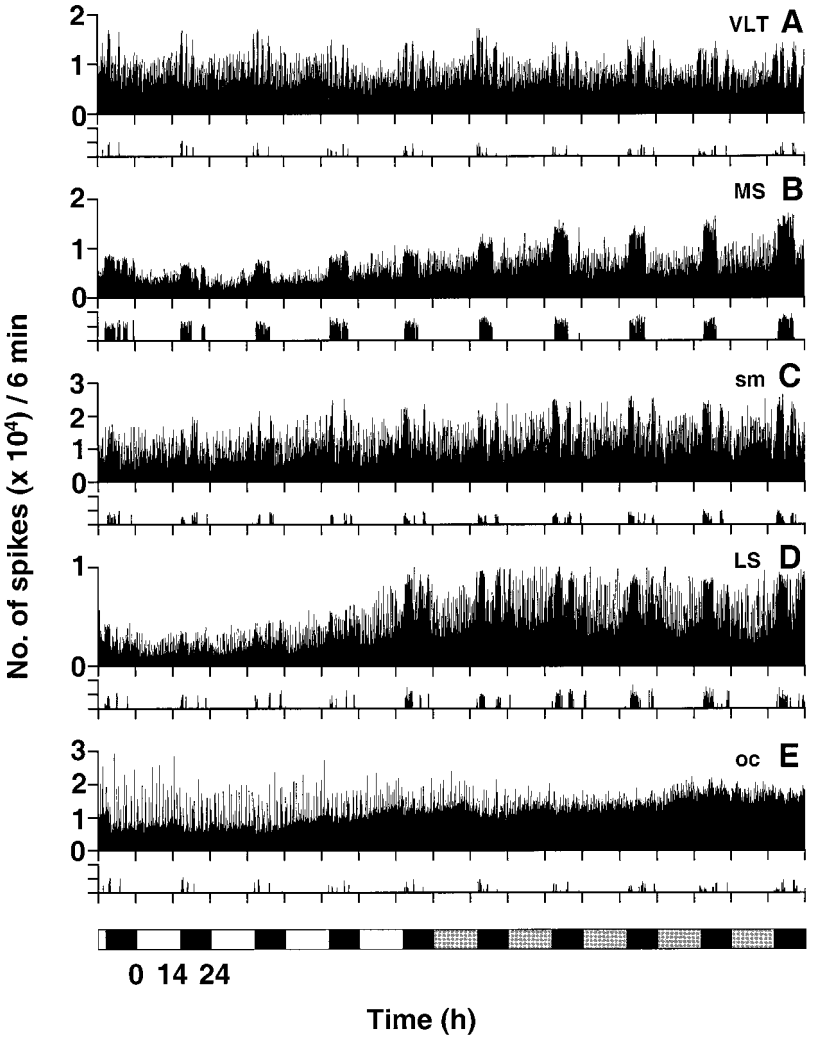

Figure 2. Daily and circadian rhythms of neural activity in several regions of the brain. MUA and locomotor activity are plotted in 6 min bins as in Figure 1. Recordings were made from the following: *A*, right side of the ventrolateral thalamic nucleus (*VLT*); *B*, right side of the medial septum (*MS*); *C*, right side of the stria medullaris (*sm*); *D*, right side of the LS; *E*, the optic chiasm (*oc*). Each plot represents a different wild-type hamster except for *A* (same animal as in *E*) and *C* (same animal as in Fig. 1*C*). Note (most clearly in *B*) that the peak of neural activity coincides with wheel-running activity.

highly effective low-cut filter (500 Hz). Using these techniques, we reduced electrical noise generated by chewing or moving to undetectable levels. Although scratching did generate detectable electrical noise, this activity was rare and did not create a problem in the analysis.

Identification of recording sites. After the electrical recordings, each hamster was anesthetized with halothane, the head amplifier was disconnected, and a small positive current (50 μA; 10 sec) was passed through the recording electrodes. The brain was removed and fixed in Zamboni's fixative solution for a few days. Frozen sections (40 μm thick) were stained with potassium ferrocyanide (5% potassium ferrocyanide in 10% HCl). Blue spots of deposited iron were used for identification of recording sites.

Data analysis. The first report of SCN neuronal recordings from freely moving rodents appeared 19 years ago and played a pivotal role in identifying the SCN as the central mammalian circadian pacemaker (Inouye and Kawamura, 1979). Since then little use has been made of this technique. A primary reason for hesitation in the use of *in vivo* recording techniques is that changes in neuronal oscillations are oftentimes difficult to identify in the raw data, and thus robust time series statistical analysis is required. No single time series analysis tool can be applied in all cases. We applied a new method, singular-spectrum analysis (SSA), in combination with older methods. Periodicities in multiunit activity (MUA) recorded *in vivo* were determined using SSA in combination with the multitaper method (MTM) approach to the fast Fourier transform (Thomson, 1982; Vautard et al., 1992).

Singular-spectrum analysis or SSA is a linear, nonparametric method based on a principal component analysis in the vector space of the delay coordinates for a times series (Elsner and Tsonis, 1996). In SSA, a single time series is expanded into a set of multivariate time series of length M, known as the "window length." M determines what range of frequencies can be resolved as a stationary signal in the calculated principal components. The principal component analysis orders the expanded time series as a new coordinate system with most information along the first coordinates. The principal components are processes of length $N - M + 1$ that can be thought of as weighted moving averages of the time series in which each accounts for a certain percentage of the total variance. SSA allows optimal detrending, identification of the noise floor in spectral estimates, and identification of intermittent oscillatory components in the data. In practice, we found that we could with reasonable success divide the data into four parts (trend variance, circadian variance, ultradian components variance, and noise variance) by use of two window lengths on the MUA data. M was set at 36 hr ($M = 360$ for 6 min bins) for the circadian time scale and 5 hr for the ultradian time scale. SSA cannot resolve periods longer than M and treats them as trends. If M is much greater than the average lifetime of an episode of oscillation, SSA cannot resolve the intermittent oscillation.

We used SSA for signal reconstruction from the noisy MUA data. Simple noise reduction by applying a fixed low-pass filter to the data is not appropriate when the spectrum is not monotonic. Because steps were taken to minimize instrument noise and a low-cut filter was used (500 Hz) before binning the impulses in the MUA data, noise is represented here mostly by random impulses from populations of neurons near the electrode. Optimal filtering of signals that are not completely stable requires methods such as Wiener filtering or SSA. Both provide optimal filters in a least squares sense. However Weiner filters arbitrarily require harmonic functions as a basis. SSA, in contrast, uses data-determined general functions that do not require any previous hypotheses about the noise variance. Unlike SSA, the Wiener method requires smooth and very reliable estimates of the power spectrum that are impossible to obtain with very short data sets. "Noise-free" circadian or ultradian time

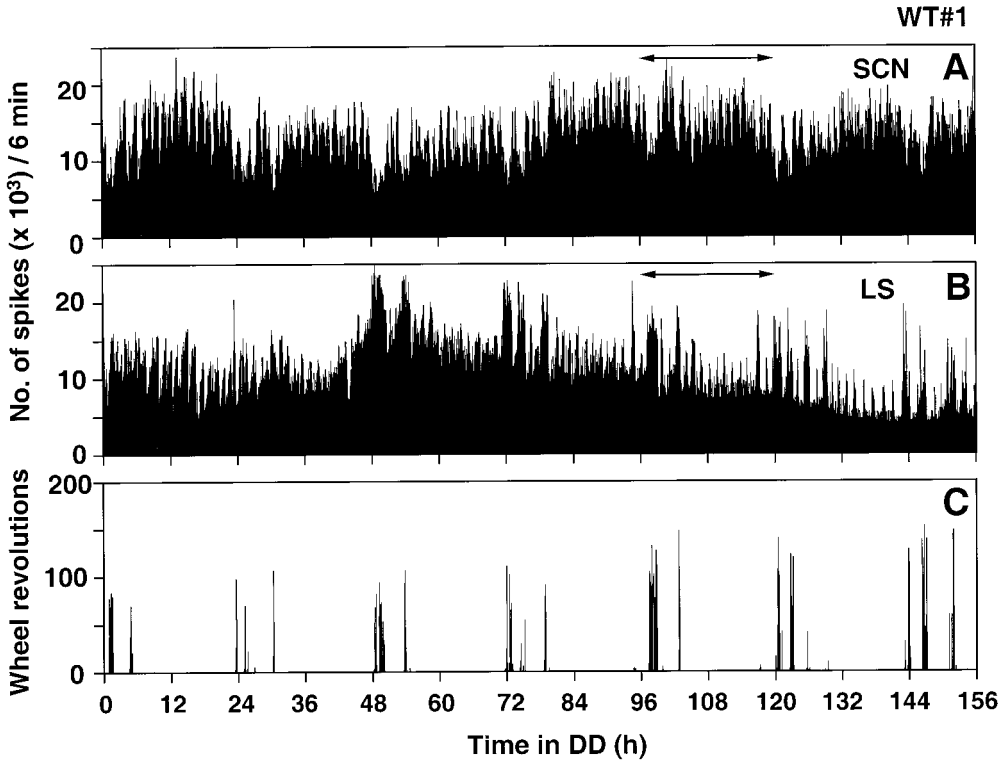

Figure 3. Wheel-running behavior and neural activity records from the SCN and LS of a wild-type hamster (*WT*) in constant darkness. Electrodes were located in the left ventromedial region of the central SCN and in the right LS. The time scale shows hours after the hamster was released into constant darkness. *A*, MUA in the SCN in 6 min bins. *B*, MUA in the LS in 6 min bins. *C*, Wheel revolutions per 6 min. The data marked by the *double-headed arrows* are presented below (see Fig. 8).

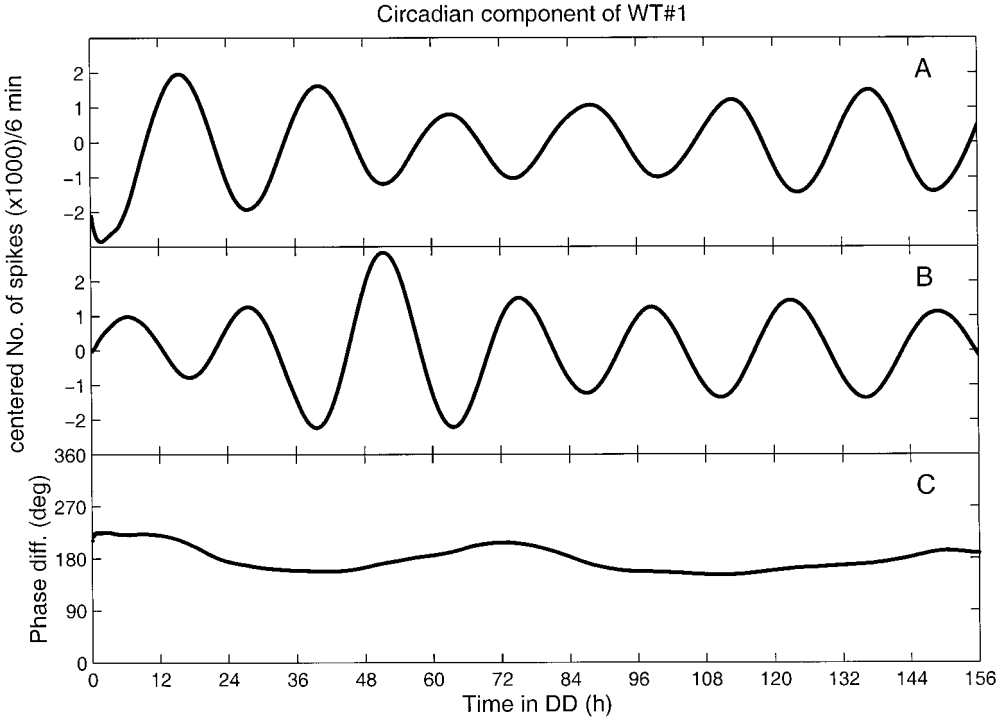

Figure 4. Mathematical analysis of the phase angle difference of the circadian rhythms recorded in the SCN and LS in a wild-type hamster. Original data are shown in Figure 3*A*,*B*. Data reconstructed by SSA for the SCN (*A*) and for the LS (*B*). *C*, Instantaneous phase angle difference between the circadian rhythms shown in *A* and *B*. The time series *A* and *B* were individually converted to their Hilbert transforms (the time series with a 90° phase shift). The resultant time series are series of complex numbers representing the original data (real part) and the Hilbert transform (imaginary part). The magnitude of each of these complex numbers is an estimate at that time of the circadian rhythm amplitude (data not shown). The angle of each of these complex numbers is an estimate at that time of the phase of the circadian rhythm relative to the beginning. The difference between the angles of *A* and *B* at each point is the instantaneous phase difference between the two circadian rhythms.

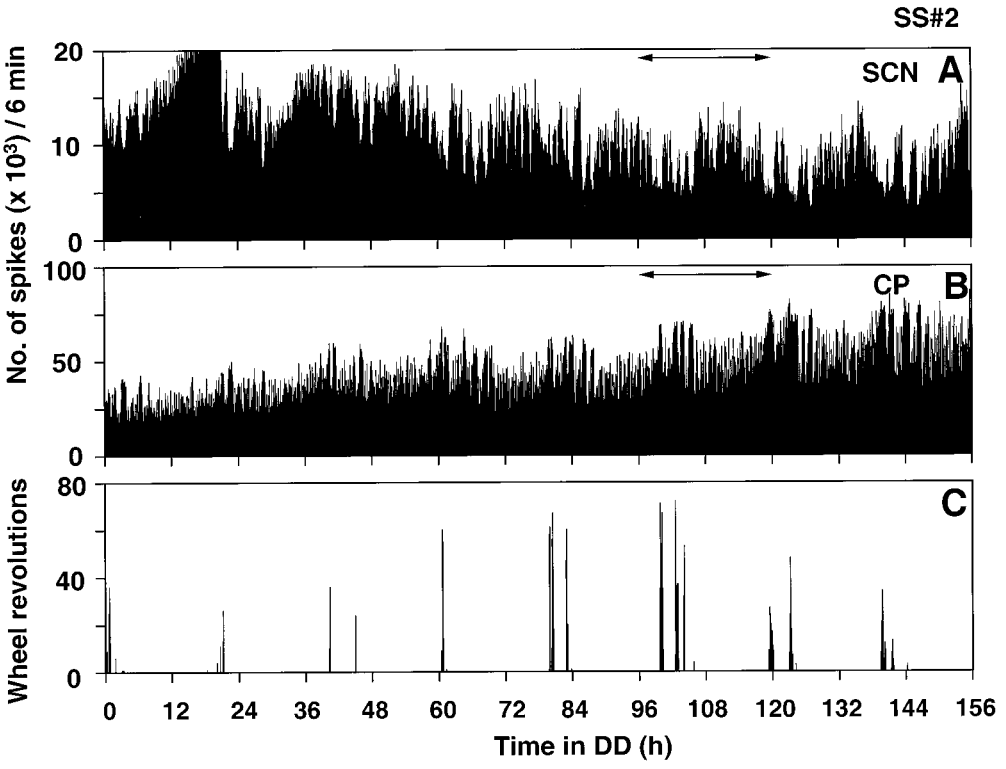

Figure 5. Wheel-running behavior and neural activity records from the SCN and CP of a *tau* mutant hamster in constant darkness. Electrodes were located in the right ventromedial part of the central region of the SCN and in the right CP. *A*, MUA in the SCN in 6 min bins. *B*, MUA in the CP in 6 min bins. *C*, Wheel revolutions per 6 min. The data marked by the *double-headed arrows* are presented below (see Fig. 10). *SS*, Homozygous *tau* mutant.

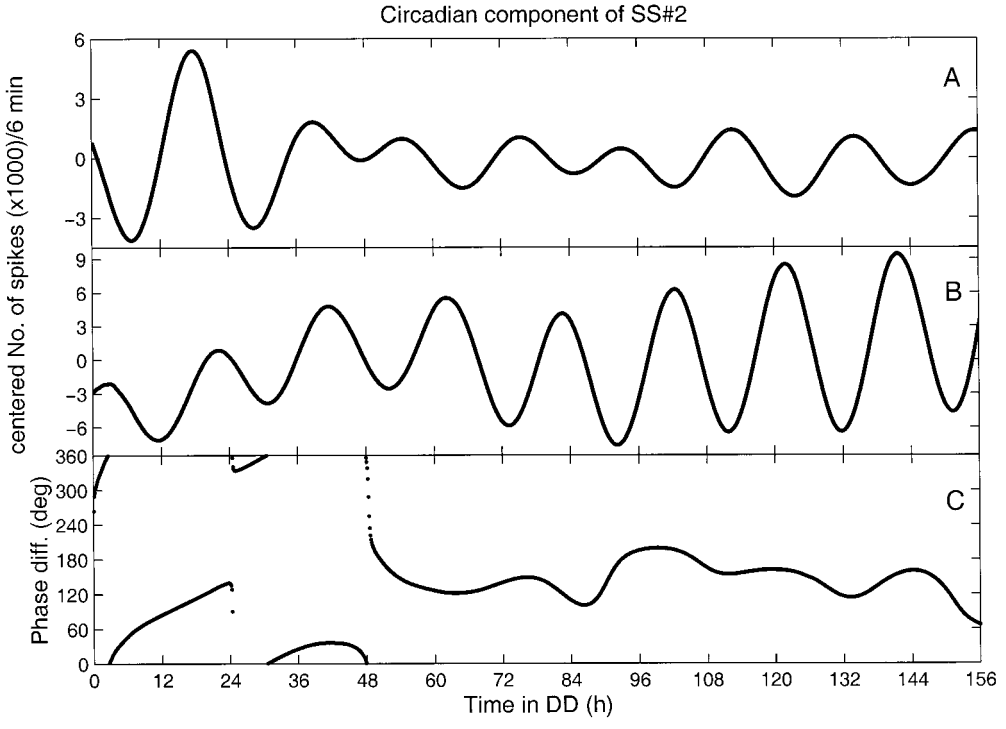

Figure 6. Mathematical analysis of the phase angle difference of the circadian rhythms recorded in the SCN and CP in a *tau* mutant hamster. Original data are shown in Figure 5. *A*, *B*, Data reconstructed by SSA for the SCN (*A*) and for the CP (*B*). *C*, Instantaneous phase angle difference between the circadian rhythms shown in *A* and *B*.

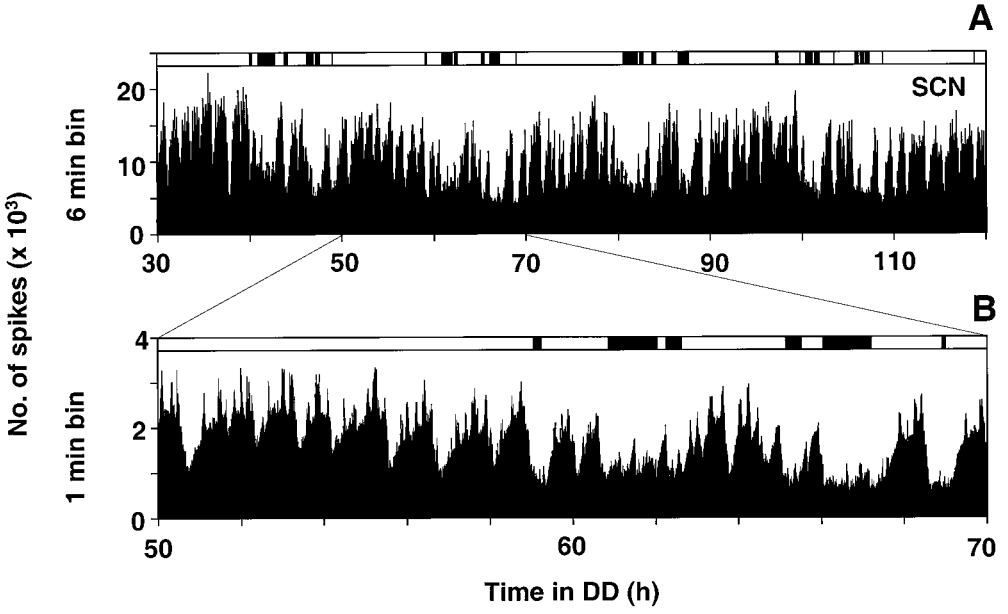

Figure 7. Circadian and ultradian rhythms of MUA in the SCN of a *tau* mutant hamster in constant darkness. In this case, the bipolar electrode became separated in the brain, with one electrode positioned on the left side and the other positioned on the right side of the ventromedial region of the caudal SCN. *Top bars* of *A* and *B* show wheel-running activity, plotted as a *black bar* when the wheel revolved more than once in 6 min. The time scale shows hours after the animal was released into constant darkness. *A*, Plot of MUA in 6 min bins. *B*, Expanded plot of 20 hr (one circadian cycle for the *tau* mutant hamster) of data from *A* with neuronal activity in 1 min bins showing ultradian rhythms of both periods as well as the negative correlation between wheel-running activity and neural activity.

series were therefore reconstructed from the SSA filters. By this method, oscillatory signals that accounted for as little as 3% of the total variance could be detected. Monte Carlo simulations assuming either white noise or correlated noise were used to evaluate the background noise level in the SSA spectra. By selecting only those principal components associated with the circadian variance of the data, we could derive an optimal (in the least squares sense) "noiseless" reconstruction of the circadian waveform in the data. Each waveform in the reconstructed time series is essentially a local fit allowing us to calculate a mean period from each animal's data set. This local noise-free fit also allowed us to determine the phase relationship as a function of time between two different locations in the brain. Periods of the ultradian rhythms were determined with one or more of the following: SSA-MTM, power spectrum estimates [e.g., maximum entropy method (MEM)], or visual inspection of the raw

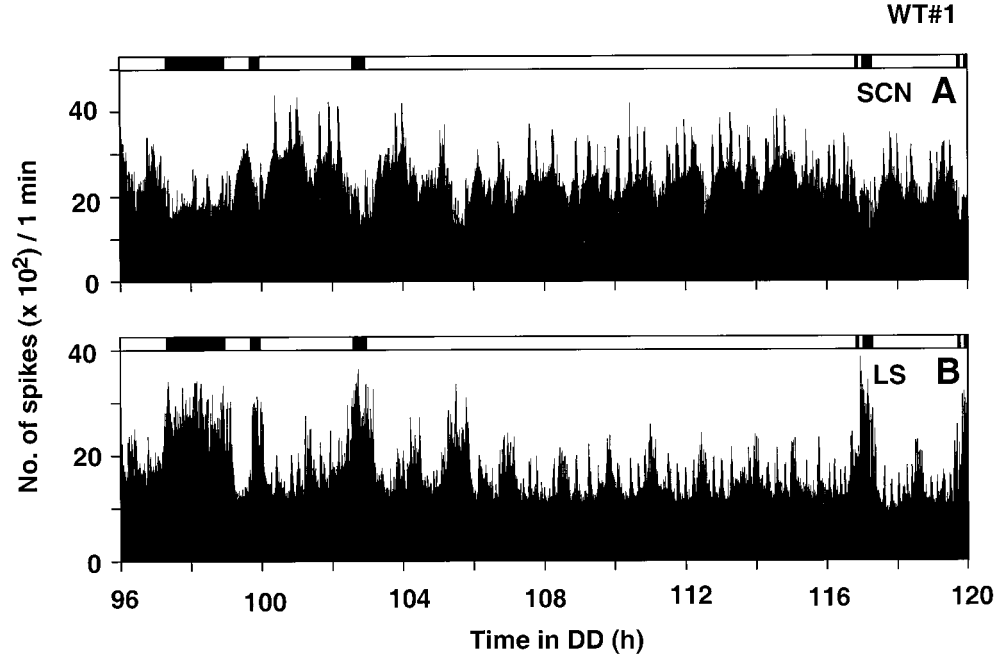

Figure 8. Ultradian rhythms in neural activity records from the SCN and LS of a wild-type hamster. *A*, Expanded plot of the 24 hr neural activity record in 1 min bins from the SCN (from Fig. 3*A*, *double-headed arrow*). The *top bar* shows wheel-running activity, plotted as a *black bar* whenever the wheel revolved more than once in 6 min. *B*, Expanded plot of the concurrent record from the LS (from Fig. 3*B*, *double-headed arrow*). Note the negative correlation of neural activity with wheel-running activity in the SCN and the positive correlation in the LS.

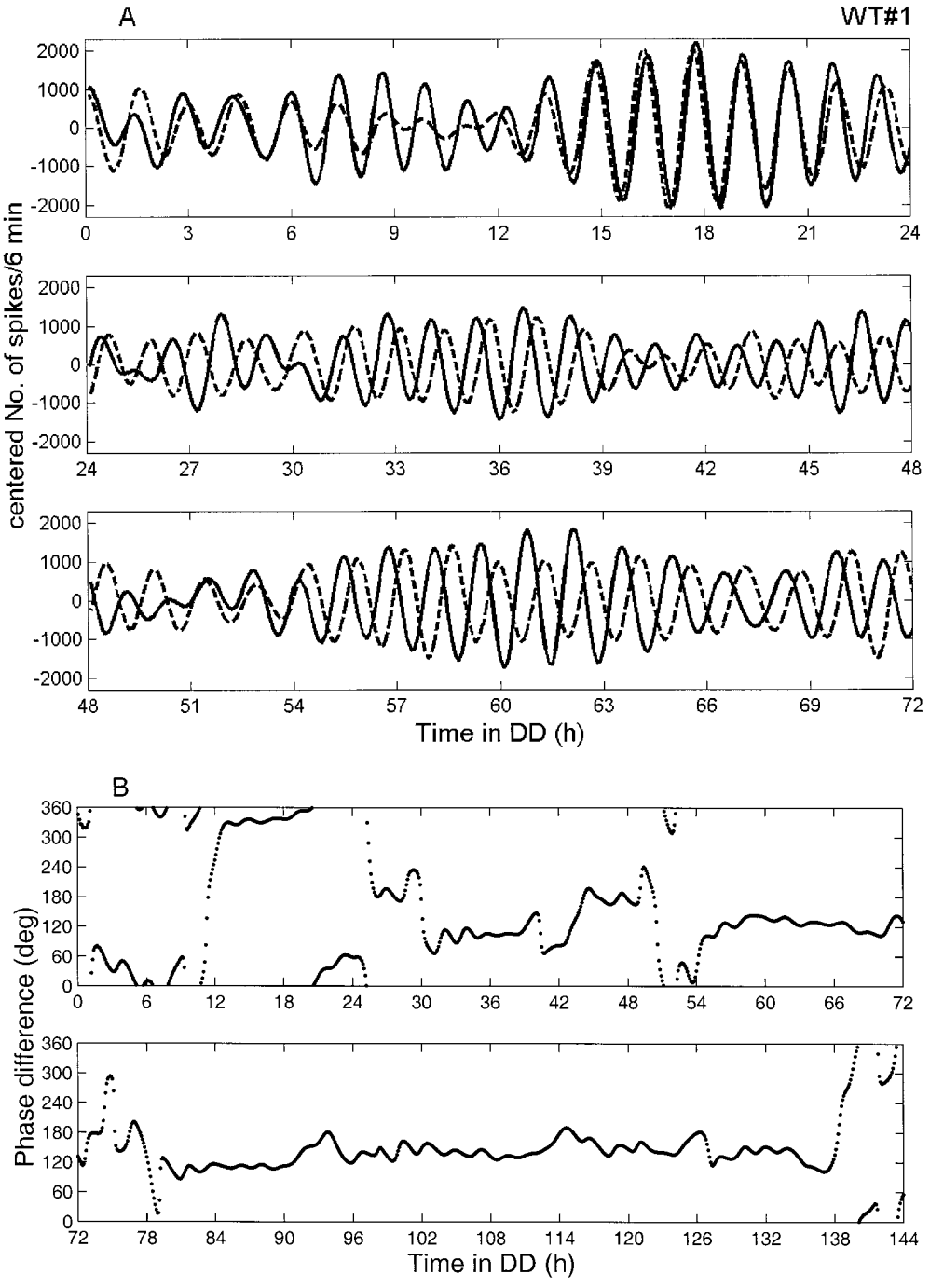

Figure 9. Mathematical analysis of ultradian rhythms recorded from the SCN and LS (from Fig. 3*A*,*B*). *A*, Data reconstructed by SSA of the 80 min ultradian rhythms in the SCN (*solid line*) and the LS (*dotted line*) for the first 72 hr of the record. *B*, Phase angle difference of the 80 min ultradian rhythms between the SCN and the LS plotted for 144 hr (see text and Fig. 4 for details).

data. MEM was performed on the data after the trend and circadian variances were removed (determined by SSA). The order of the MEM (*M*, number of poles in the autoregressive model) was kept much lower than the number of data points and varied over the range to monitor stability of peaks of interest in the spectrum (M, 20–60; $N > 1600$). MEM is fully consistent with SSA so that the additive property of the spectra is conserved exactly (Vautard et al., 1992). Periods of very short ultradian rhythms were determined by visual inspection; areas of high-frequency ultradian activity were measured for the average period, and measurements from six areas per animal were averaged to obtain the period. The periods of the wheel-running activity were obtained by using a standard chi-square periodogram for comparison with the other methods (see Table 1).

Phase analysis. We used the discrete Hilbert transform of the SSA-reconstructed waveforms to estimate the instantaneous phase difference between the oscillations inside and outside the SCN. The Hilbert transform is the imaginary part of the analytical signal of a real time series (Bendat and Piersol, 1986). An estimate of the imaginary part from the real part of the time series can be calculated by assuming the signal is causal (a sequential time series) and by using the inverse of a one-sided Fourier transform (fast Fourier transform coefficients that correspond to negative frequencies are set to zero before doing the inverse transform). The

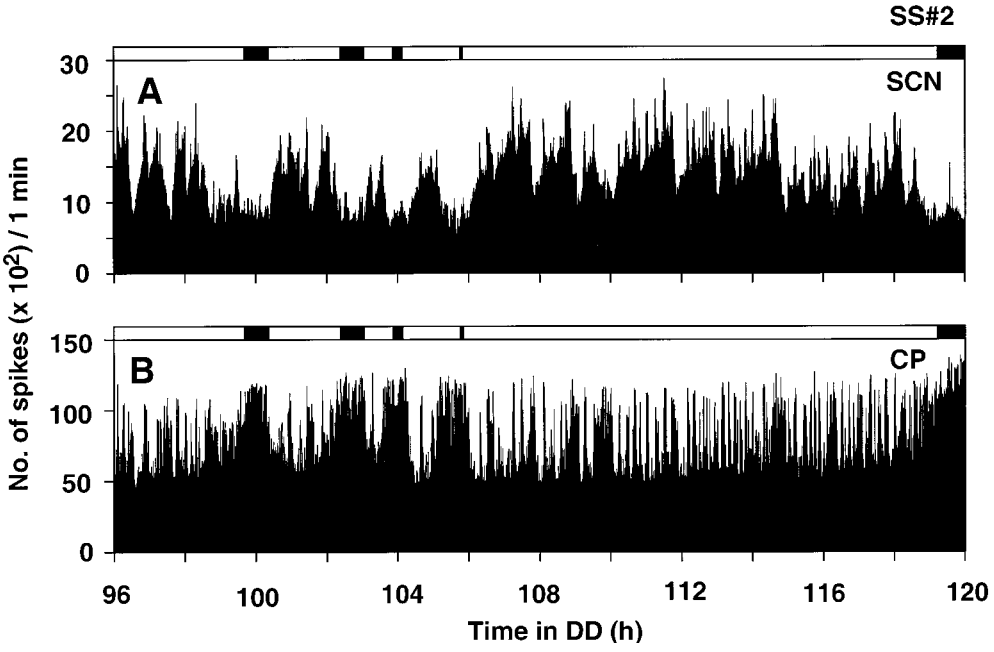

Figure 10. Ultradian rhythms in neural activity records from the SCN and CP in a *tau* mutant hamster. *A*, Expanded plot of 24 hr neural activity in 1 min bins from the SCN (from Fig. 5*A*, *double-headed arrow*). The *top bar* shows wheel-running activity, plotted as a *black bar* whenever the wheel revolved more than once in 6 min. *B*, Expanded plot of the concurrent record from the CP (from Fig. 5*B*, *double-headed arrow*). Note the positive (*CP*) and negative (*SCN*) correlations with wheel-running behavior.

resultant time series is phase shifted 90° from the original time series. This process is sensitive to noise and requires a filtered input such as that provided by SSA. The temporal change in the relative phase between the oscillations recorded in different brain regions was examined using this method. Circular statistics were used to compute the mean phase difference for the circadian rhythms in different brain regions (Fisher, 1995).

Experimental protocols. To observe daily and circadian changes of neural activity in and outside of the SCN, we recorded MUA from 20 wild-type hamsters implanted with two electrodes. One electrode was directed into the SCN, and the other was aimed at one of several regions outside of the SCN. Animals were recorded for 4 d in a light/dark cycle (14:10 hr LD; light intensity of ~300 lux at cage level), followed by 6 d in constant darkness (DD). To evaluate the effects of the *tau* mutation on the rhythmic properties, we recorded MUA from 10 wild-type and 14 *tau* mutant hamsters implanted with two electrodes, one aimed at the SCN and the other at one of the following sites: the lateral septum (LS), the caudate putamen (CP), the ventrolateral region of the thalamus, and the bed nucleus of the stria terminalis (BNST). These hamsters were placed into DD at the time of their normal lights off, and MUA was recorded for 7 d. We only used data from implantations in which both wires of each electrode were located in the same nucleus. We sometimes observed one wire located in the SCN, while the other was in the surrounding area; in those cases the data were discarded.

RESULTS

Circadian rhythms both within and outside the SCN

MUA recorded in the SCN showed clear daily (LD) and circadian (DD) rhythms (Fig. 1). Peak impulse frequency of these rhythms always occurred at the middle of the day (LD) or subjective day (DD), in antiphase with the hamster's nocturnal wheel-running activity. The amplitude of the neuronal activity rhythms varied from experiment to experiment and was not strongly correlated

Table 1. Summary of circadian and ultradian periods

		Neural activity in the SCN		
	Wheel-running activity (hr)	Circadian (hr)	Ultradian 1 (min)	Ultradian 2 (min)
WT#1	24.3	24.5	84	14
WT#2	24.2	24.1	75	14
WT#3	23.9	23.8	87	14
WT#5	24.2	24.1	76	15
Mean ± SE	24.15 ± 0.09	24.13 ± 0.14	80.5 ± 3.0	14.3 ± 0.3
SS#2	19.8	19.7	75	15
SS#4	20.1	20.3	78	15
SS#5	20.0	20.1	99	12
SS#7	19.8	19.7	71	15
Mean ± SE	19.93 ± 0.08	19.95 ± 0.15	80.8 ± 6.3	14.3 ± 0.8
Two-tailed *t* test	$p < 0.0005$	$p < 0.0005$	$p = 0.97$	$p = 1.00$

Seven days of MUA and wheel-running activity were collected simultaneously in constant darkness (WT, wild type; SS, homozygous *tau* mutants). Periods of wheel-running rhythms were obtained by chi-square periodogram. Periods of circadian and ultradian 1 rhythms of MUA were determined by SSA. Periods of ultradian 2 rhythms were determined by visual inspection. (See text for details of analysis methods.)

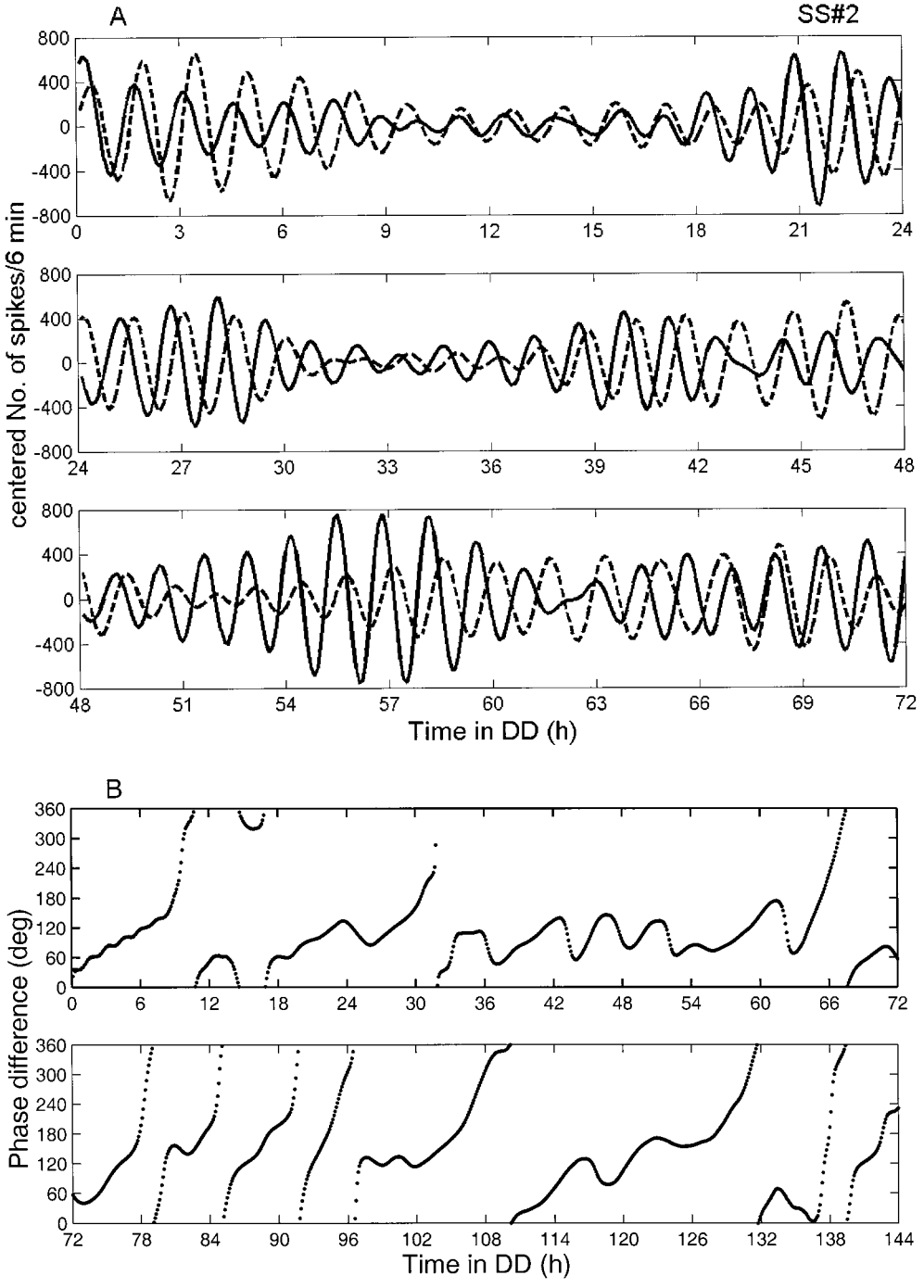

Figure 11. Mathematical analysis of the ultradian rhythms recorded from the SCN and CP in a *tau* mutant hamster. *A*, Data reconstructed by SSA of the 80 min ultradian rhythms in the SCN (*solid line*) and the CP (*dotted line*) for the first 72 hr of the record. *B*, Phase angle difference of the 80 min ultradian rhythms between the SCN and the CP plotted for 144 hr (see text and Fig. 4 for details).

with the recording site, although recordings obtained in the ventral portion of the SCN tended to have a higher amplitude than did those from the dorsal portion. Although the recording sites were nearly identical for the animals whose records are shown in Figure 1, *B* and *C*, the MUA displayed in Figure 1*B* has higher average amplitude oscillations than does that in Figure 1*C*. SSA detected a significant circadian (or daily) oscillation with a centered amplitude of ~10,000 spikes per 6 min interval from the data plotted in Figure 1*B*. The centered amplitude from data shown in Figure 1*C* was approximately one-fourth as large.

There was no consistent relationship between overall levels of locomotor activity and MUA activity. For example, the wheel-running activity of animals shown in Figure 1, *A* and *B*, was quite variable (on some nights the hamsters ran much more than on others), yet the amplitude of the MUA rhythms remained relatively constant. Furthermore, in all three examples in Figure 1, the amplitude of MUA oscillation in the SCN did not change when the animals were released from LD into DD. Even in the case of the animal whose data are shown in Figure 1*A*, in which the electrode was located in the lateral portion of the SCN (which

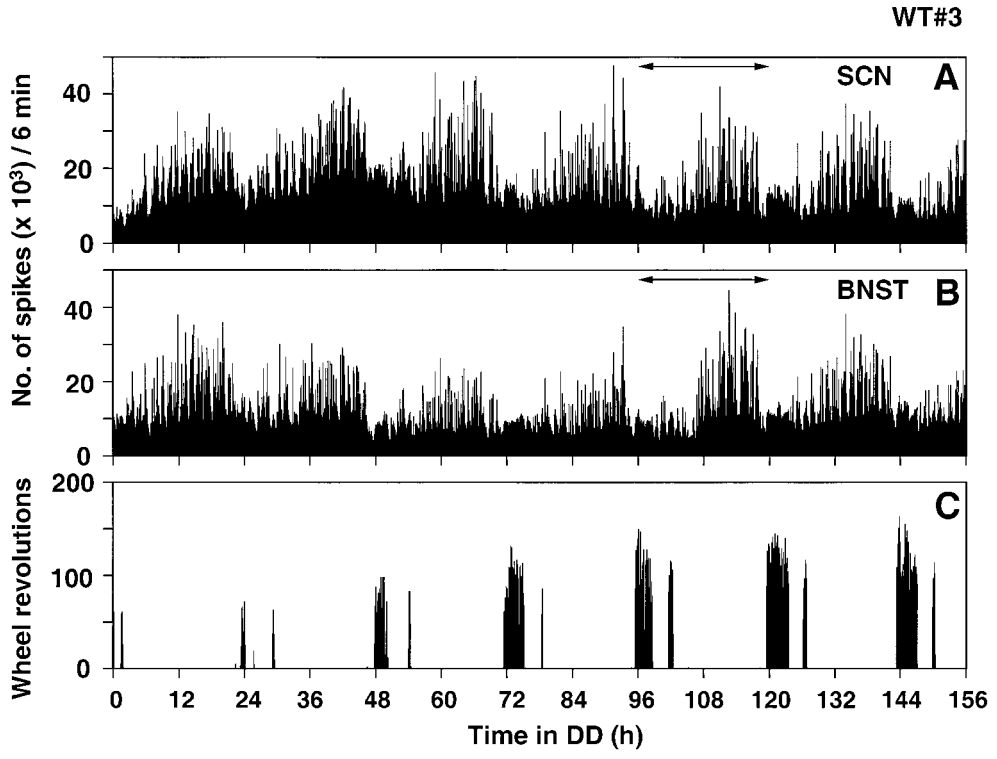

Figure 12. Neural activity records obtained simultaneously from the SCN and the BNST in a wild-type hamster in constant darkness. Electrodes were located in the right ventromedial portion of the central SCN and in the right anteromedial portion of the BNST. *A*, MUA in the SCN in 6 min bins. *B*, MUA in the BNST in 6 min bins. *C*, Wheel revolutions per 6 min. The data marked by the *double-headed arrows* are presented below (see Fig. 14). Note the almost perfect phase lock between these two regions and that both are in antiphase with wheel running.

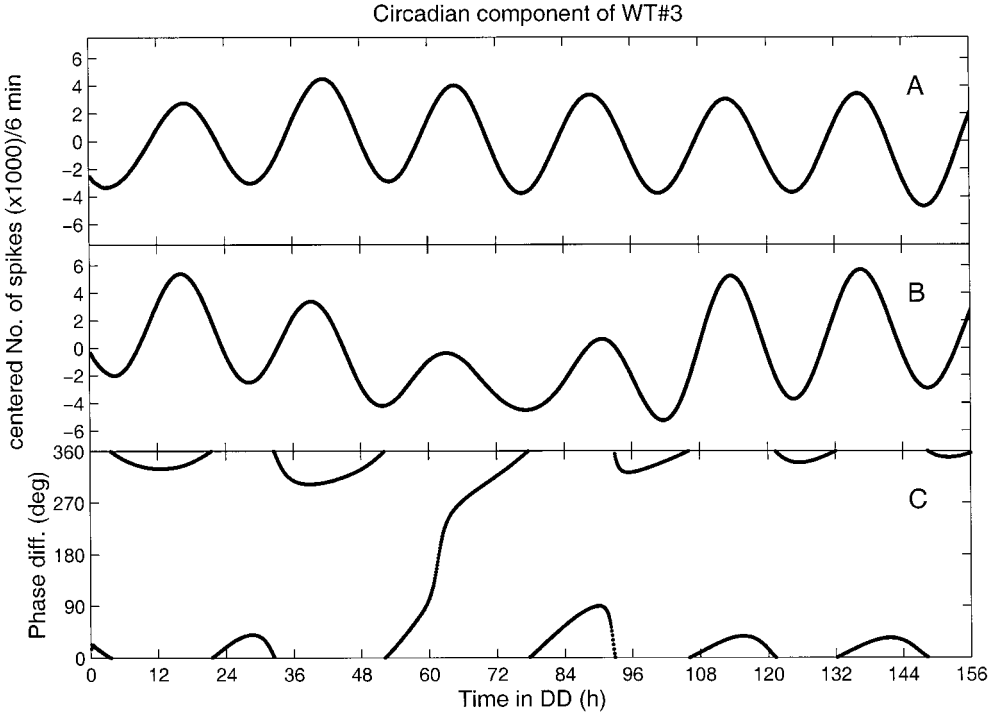

Figure 13. Mathematical analysis of the phase angle difference of the circadian rhythms recorded in the SCN and the BNST in a wild-type hamster (original data in Fig. 12). *A*, *B*, Data reconstructed by SSA for the SCN (*A*) and for the BNST (*B*). *C*, Instantaneous phase angle difference between the circadian rhythms shown in *A* and *B* (see text and Fig. 4 for details).

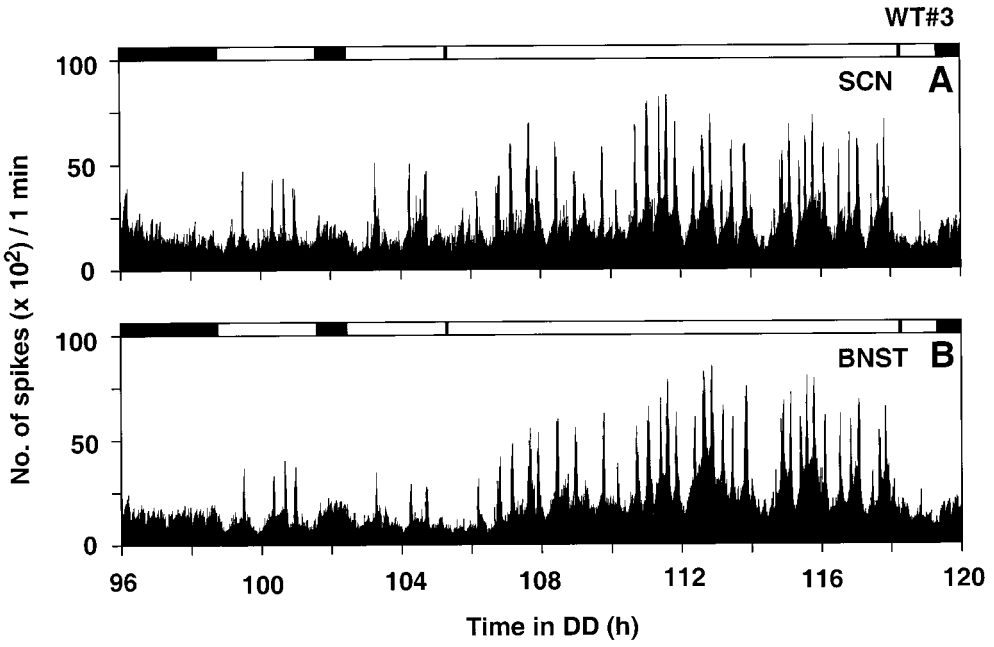

Figure 14. Ultradian rhythms of neural activity recorded from the SCN and the BNST in a wild-type hamster. *A*, Expanded plot of 24 hr neural activity record in 1 min bins from the SCN (from Fig. 12*A*, *double-headed arrow*). The *top bar* shows wheel-running activity, plotted as a *black bar* whenever the wheel revolved more than once in 6 min. *B*, Expanded plot of 24 hr neural activity record in 1 min bins from the BNST (from Fig. 12*B*, *double-headed arrow*). Note that both the 80 and 14 min ultradian rhythms are usually in-phase.

receives the retinal projection), light did not have an acute effect on the MUA.

Most regions outside of the SCN also showed clear daily or circadian rhythms (Fig. 2). The ventrolateral thalamic nucleus ($n = 3$), the CP ($n = 3$), the accumbens nucleus ($n = 1$), the medial septum ($n = 1$), the LS ($n = 6$), the ventromedial hypothalamic nucleus ($n = 2$), the medial preoptic region ($n = 1$), and the stria medullaris ($n = 3$) all exhibited circadian rhythms with peak impulse activity occurring at night or subjective night that, unlike the electrical activity rhythm in the SCN, was in-phase with locomotor activity. SSA of activity in the optic chiasm ($n = 2$) revealed no circadian components, but ultradian rhythms were present and were stronger in LD than in DD.

There were clear correlations between electrical activity in the SCN and in other brain regions. The data in Figure 3 were recorded from a wild-type hamster in DD. MUA from the SCN (Fig. 3*A*) and the LS (Fig. 3*B*) and wheel-running activity (Fig. 3*C*) were collected simultaneously; all three data sets contain significant circadian components. Figure 4 presents reconstructed waveforms of the circadian components using the SSA method. Circadian rhythms in the SCN (Fig. 4*A*) and LS (Fig. 4*B*) were tightly locked in an antiphase relationship (Fig. 4*C*). Their periods were matched to that of the wheel-running activity rhythm that was in antiphase to the SCN. The data in Figure 5 were recorded from a *tau* mutant hamster. MUA was recorded from the SCN (Fig. 5*A*) and CP (Fig. 5*B*). Both regions showed significant circadian rhythms that matched the 20 hr period of the wheel-running rhythm (Fig. 5*C*). The phase angle difference between these two brain regions was also stable in antiphase (Fig. 6; sometimes, as in this example, stable phase relationships did not develop the first cycle or two of constant darkness). Other examples (SCN and LS in a wild type, $n = 1$; SCN and ventrolateral thalamus in a wild type, $n = 1$; and SCN and ventrolateral thalamus in a *tau* mutant, $n = 1$) showed similar phase relationships.

Ultradian rhythms

MUA in the SCN and in other brain regions displayed ultradian components in addition to circadian ones. We succeeded in identifying a significant circadian component and two ultradian components from the time series data in all brain regions analyzed. Figure 7 shows an example of MUA recorded from the SCN in a *tau* mutant hamster in DD. As expected, an ~20 hr circadian component in antiphase to the wheel-running activity rhythm was present. The record also shows a clear ultradian component with a period of ~80 min. Furthermore, in expanded plots we could detect a higher frequency rhythm of ~14 min that was most clearly expressed around the peak of the 80 min oscillation.

Expanded plots of 24 hr segments recorded from the SCN (Fig. 3*A*) and the LS (Fig. 3*B*) of a wild-type hamster are shown in Figure 8, *A* and *B*, respectively. These data contain two ultradian components, ~80 and ~14 min. The two components were identified by spectral analysis and visual inspection, respectively. The time domain SSA reconstructions of the ~80 min ultradian oscillations in the SCN and the LS were in-phase with each other on the first day after transfer from LD to DD; however by the second day in DD they had shifted to an antiphase relationship (Fig. 9*A*,*B*). The ~14 min ultradian rhythms appeared to be in-phase between the SCN and the LS (Fig. 8). We obtained similar results from two other wild-type hamsters (recorded from the SCN and the ventrolateral thalamus or LS).

The ultradian components recorded from *tau* mutant hamsters also had periods of ~80 and ~14 min. Time series analysis and visual inspection of simultaneous recordings from the SCN and the CP in a *tau* mutant hamster revealed these two ultradian components (Fig. 10). In this data set the phase relationships of

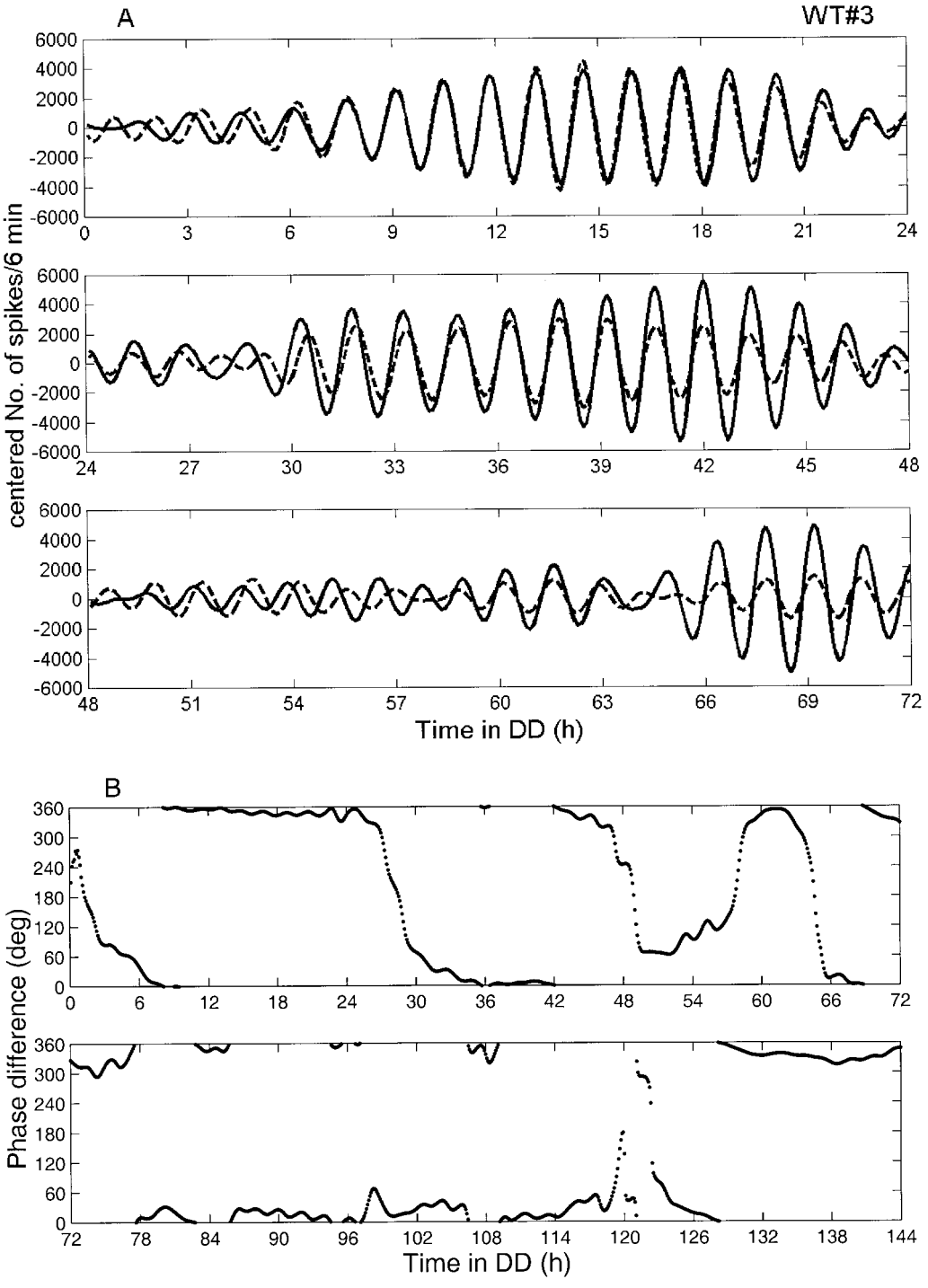

Figure 15. Mathematical analysis of the ultradian rhythms recorded from the SCN and the BNST in a wild-type hamster. *A*, Data reconstructed by SSA of the 80 min ultradian rhythms in the SCN (*solid line*) and the BNST (*dotted line*) for the first 72 hr of the record. *B*, Phase angle difference of the 80 min ultradian rhythms between the SCN and the BNST plotted for 144 hr (see text and Fig. 4 for details).

the 80 min oscillations in the two areas were often in antiphase, but their phase relationship was much less stable than in similar recordings from wild types (Fig. 11). As in wild types, the ~14 min rhythms always appeared to be in-phase (Fig. 10). A second *tau* mutant hamster in which electrical recordings were obtained from the SCN and the ventrolateral thalamus exhibited similar properties.

Effects of the *tau* mutation on the circadian and ultradian periods of MUA

The period of the rhythm of wheel-running activity in wild-type hamsters was ~24 hr and closely matched the circadian component of the electrical activity in the SCN. To assess the effect of the *tau* mutation on the rhythmic properties in the SCN, we obtained four 1-week-long recordings for analysis of the period of

the rhythm in DD. The ~20 hr period of wheel-running rhythms in *tau* mutants closely matched the circadian MUA rhythms in the SCN. There were no significant differences between wild type and *tau* mutants in the periods of the ultradian components (80 and 14 min). The variation in frequency among animals within each genotype was as great as that between genotypes (Table 1).

Effect of wheel running on MUA

Locomotor activity affects the expression of MUA in the SCN and elsewhere in the brain. MUA in the SCN was decreased during wheel running, whereas MUA in other areas was enhanced (Figs. 1–3, 5, 7, 8, 10). These changes in the levels of MUA were precisely correlated with locomotor activity and were more pronounced the more vigorously the animals ran in their wheels.

Phase of MUA in the BNST

In contrast to MUA from all other recording sites outside of the SCN, MUA recorded from the anteromedial part of the BNST exhibited oscillations (circadian and ultradian) in-phase with the SCN (Figs. 12, 13, 14, 15). As seen in the SCN and again in contrast to that seen at other sites, neural activity in the BNST was suppressed during wheel running (Figs. 12, 14). We also observed similar phase relationships in one recording from the posteromedial part of the BNST of a wild-type animal and from the anteromedial part of the BNST in one *tau* mutant.

DISCUSSION

Circadian rhythms in electrical activity

Inouye and Kawamura (1979) reported that the MUA in the SCN recorded from freely moving rats displayed a circadian rhythm with peak impulse frequency occurring during the day. They also recorded MUA circadian rhythms from regions outside the SCN that exhibited peak activity at night, out-of-phase with the SCN rhythm and in-phase with the animal's locomotor activity. Because MUA in the SCN remained rhythmic after the nucleus was isolated (within a hypothalamic island), while the rhythms outside of the SCN disappeared, they concluded that the circadian pacemaker was in the SCN and that rhythms outside the SCN were being driven (in antiphase) by the SCN (Inouye and Kawamura, 1982). Later, Yamazaki et al. (1994) showed that the circadian rhythm of ATP content in the SCN of rats is also in antiphase with this rhythm in the anterior hypothalamus and CP. Our results with hamsters are in good general agreement with the results in rats. We find that the circadian rhythms of MUA within the SCN are out-of-phase with those recorded from brain areas outside the SCN, with the important exception of the BNST, an area from which Inouye and Kawamura did not record.

We found that the period of the circadian rhythm in MUA both within and outside of the SCN was affected as expected by the *tau* mutation and matched the period of wheel-running behavior both in wild-type hamsters (~24 hr) and in *tau* mutants (~20 hr). Davies and Mason (1994) reported a circadian electrical activity rhythm with a period of ~20 hr from *tau* mutant SCN in acute slice preparation that was monitored for 36 hr. Liu et al. (1997) reported that circadian periodicities of electrical activity in SCN cells dispersed in cell culture from homozygous, heterozygous, and wild-type hamsters exhibit free-running periods that correlate with their genotype. Our results obtained *in vivo* confirm that the altered period of neuronal activity is expressed within the SCN of intact *tau* mutant hamsters. The correspondence of the *in vivo* with the *in vitro* results provides important confirmation of the usefulness of the *in vitro* model. We know that at least the normal period of the intact SCN is conserved in the dish.

The genetically determined period of the SCN is also conserved in transplantation experiments in which the locomotor rhythms restored by transplanted SCN tissue have the periods determined by the genotype of the donor not the host (Ralph et al., 1990; Vogelbaum and Menaker, 1992; Silver et al., 1996). However, the data of Silver et al. (1996) suggest strongly that in the transplant experiments the link between the transplanted tissue and the host's locomotor system is hormonal not neural. Therefore, although the several studies of SCN rhythmicity using *in vitro*, transplant, and *in vivo* methods are consistent, they leave open questions about the functional connections of the SCN with the motor control system. In particular, it will be important to determine the roles of both neural and humoral SCN outputs in controlling locomotor behavior in intact animals.

Ultradian rhythms

MUA from the SCN exhibited two different, clearly discernable ultradian components after several days in constant darkness. The 80 min ultradian rhythm was out-of-phase with other brain regions (except the BNST in which all rhythms were always in-phase with those in the SCN). However, immediately after transfer from LD to DD, the 80 min rhythms within and outside the SCN were temporarily in-phase. In the *tau* mutant, these rhythms sometimes ran independently. This suggests that 80 min ultradian pacemakers may be located both in and outside of the SCN and that the light/dark cycle may influence their phase relationships. A similar ultradian rhythm can be observed in figures published by Kawamura and Inouye (1979; their Fig. 5) and Inouye and Kawamura (1982; their Fig. 7), which show data from MUA recorded in rat within a hypothalamic island containing the SCN as well as outside of the island. That observation supports the idea that ultradian periodicities are generated from sites both within and outside the SCN. Recently, Meijer et al. (1997) found significant ultradian periods of 4 hr and 170, 130, and 100 min in rat SCN *in vivo* and a significant period of 3.5 hr in rat SCN *in vitro*. MUA from optic chiasm in hamster and rat (Inouye and Kawamura, 1979; Omata and Kawamura, 1988) has been reported to contain circadian components. However, in our recordings we observed only ultradian rhythms from this site.

The source and mechanism for the generation of ultradian periodicities within the brain are obscure, and there are many possible candidates [e.g., in the posterior hypothalamic area of the conscious rat, the release rates of the catecholamines and histamine fluctuate with the following periods: histamine, 83 min; dopamine and noradrenaline, 92 min; and adrenaline, 99 min (Dietl et al., 1992; Prast et al., 1992; Grass et al., 1996)].

Very short (~14 min) ultradian rhythms were present in all brain regions from which we recorded. Although not observable by our spectral analysis methods because of limitations in sampling frequency resolution and signal frequency variability, this periodicity was easily detectable visually in displays of the recordings. The rhythm was in-phase among all brain regions. The ~14 min period is significantly longer than an ultradian periodicity reported previously by Miller and Fuller (1992), who observed rhythms with periods of ~120 sec that were lengthened by retinal illumination in urethane-anesthetized rats.

We failed to find any differences in the periods of ultradian rhythms of *tau* mutant and wild-type hamsters, even though the circadian periodicity of the *tau* mutant is shortened by >15 percent. This suggests that the *tau* mutation may affect circadian

but not ultradian rhythms of MUA. This is in contrast to its effect on luteinizing hormone pulsatility (Loudon et al., 1994) and to the effect of mutations in the *per* gene in *Drosophila* that alter the periods of both circadian rhythms and high-frequency neural rhythms involved in the control of the courtship song (Kyriacou, 1990). However, our data do suggest that ultradian rhythms of MUA in *tau* mutants may have more variable periods and phase relationships than do those in wild types, although we are presently unable to quantify this difference.

Bed nucleus rhythmicity

Unexpectedly, and uniquely among all sites in which recordings have been made, the circadian rhythm of electrical activity in the BNST is in-phase with the SCN electrical activity rhythm. In a previous study Inouye (1983) recorded MUA from seven regions of the rat brain (not including the BNST), but only the SCN showed a circadian rhythm that peaked during the day; rhythms from all the other sites peaked at night. In our recordings, ultradian rhythms in the BNST were also in-phase with those in the SCN. Cross-spectral estimates suggest that the BNST and SCN are tightly coupled to each other (data not shown).

There is anatomical evidence that SCN efferent pathways reach the BNST (Kalsbeek et al., 1993; Morin et al., 1994). However, it does not appear that the BNST projects to the SCN (Numan and Numan, 1996). The BNST may therefore be part of an output pathway from the SCN to locomotor centers. This would be completely consistent with our data. The BNST is a complex nucleus with several subdivisions; it has been reported to be involved in the control of photoperiod measurement (Raitiere et al., 1995), maternal behavior (Numan and Numan, 1996), and mating behavior (Wood and Newman, 1993), all of which may be influenced by the circadian system. Our preliminary data from lesion studies suggest that the BNST may be involved in controlling the level and pattern of locomotor activity (Yamazaki et al., 1997).

Effects of locomotor activity on SCN electrical activity

Our data demonstrate that an animal's movements affect electrical activity in several brain areas. Wheel-running activity acutely decreased SCN (and BNST) neural activity and enhanced neural activity outside the SCN (see also Meijer et al., 1997). Although we were not able to determine the causal relationship involved (i.e., does increased activity in extra-SCN regions lead to inhibition of SCN activity or vice versa?), we believe that this finding has great potential significance. It is intriguing to speculate that reductions in SCN neural activity associated with locomotor activity may underlie the "nonphotic" phase shifts of circadian rhythms that are produced by vigorous wheel running (Reebs and Mrosovsky, 1989).

The work reported here represents a level of analysis of mammalian circadian organization that has been almost completely neglected since it was pioneered by Inouye and Kawamura 20 years ago. Technical and conceptual advances over the past two decades have made it more tractable, although it is still labor intensive. In spite of the inherent difficulty of obtaining it, knowledge of the dynamics of electrical activity in the several brain regions controlling circadian behavior in intact, unanesthetized animals is likely to be essential for an understanding of this important regulatory system.

REFERENCES

Bendat JS, Piersol AG (1986) The Hilbert transform. In: Random data: analysis and measurement procedures, 2nd Edition, pp 484–516. New York: Wiley.

Bergman H, Feingold A, Nini A, Raz A, Slovin H, Abeles M, Vaadia E (1998) Physiological aspects of information processing in the basal ganglia of normal and Parkinsonian primates. Trend Neurosci 21:32–38.

Bos NPA, Mirmiran M (1990) Circadian rhythms in spontaneous neuronal discharges of the cultured suprachiasmatic nucleus. Brain Res 511:158–162.

Davies IR, Mason R (1994) *Tau*-mutant hamster SCN clock neurons express a 20 h firing rate rhythm *in vitro*. NeuroReport 5:2165–2168.

Dietl H, Prast H, Philippu A (1992) Pulsatile release of catecholamines in the hypothalamus of conscious rats. Naunyn Schmiedebergs Arch Pharmacol 347:28–33.

Edgar DM, Martin CE, Dement WC (1991) Activity feedback to the mammalian circadian pacemaker: influence on observed measures of rhythm period length. J Biol Rhythms 6:185–199.

Elsner JB, Tsonis AA (1996) Singular spectrum analysis: a new tool in time series analysis. New York: Plenum.

Fisher NI (1995) Statistical analysis of circular data. Cambridge, UK: Cambridge UP.

Grass K, Prast H, Philippu A (1996) Influence of mediobasal hypothalamic lesion and catecholamine receptor antagonists on ultradian rhythm of EEG in the posterior hypothalamus of the rat. Neurosci Lett 207:93–96.

Green DJ, Gillette R (1982) Circadian rhythm of firing rate recorded from single cells in the rat suprachiasmatic brain slice. Brain Res 245:198–200.

Groos G, Hendricks I (1982) Circadian rhythms in electrical discharge of rat suprachiasmatic neurons recorded *in vitro*. Neurosci Lett 34:283–288.

Herzog ED, Geusz ME, Khalsa SBS, Straume M, Block GD (1997) Circadian rhythms in mouse suprachiasmatic nucleus explants on multimicroelectrode plates. Brain Res 757:285–290.

Inouye S-IT (1983) Does the ventromedial hypothalamic nucleus contain a self-sustained circadian oscillator associated with periodic feedings? Brain Res 279:53–63.

Inouye S-IT, Kawamura H (1979) Persistence of circadian rhythmicity in a mammalian hypothalamic "island" containing the suprachiasmatic nucleus. Proc Natl Acad Sci USA 76:5962–5966.

Inouye S-IT, Kawamura H (1982) Characteristics of a circadian pacemaker in the suprachiasmatic nucleus. J Comp Physiol [A] 146:153–160.

Kalsbeek A, Teclemariam-Mesbah R, Pevet P (1993) Efferent projections of the suprachiasmatic nucleus in the golden hamster (*Mesocricetus auratus*). J Comp Neurol 332:293–314.

Kawamura H, Inouye S-IT (1979) Circadian rhythm in a hypothalamic island containing the suprachiasmatic nucleus. In: Biological rhythms and their central mechanism (Suda M, Hayaishi O, Nakagawa H, eds), pp 335–341. Amsterdam: Elsevier Science.

Klein DC, Moore RY, Reppert SM (1991) Suprachiasmatic nucleus: the mind's clock. New York: Oxford UP.

Kyriacou CP (1990) The molecular ethology of the *period* gene in *Drosophila*. Behav Genet 20:191–211.

Lehman MN, Silver R, Gladstone WR, Kahn RM, Gibson M, Bittman EL (1987) Circadian rhythmicity restored by neural transplant: immunocytochemical characterization of the graft and its integration with the host brain. J Neurosci 7:1626–1638.

Liu C, Weaver DR, Strogatz SH, Reppert SM (1997) Cellular construction of a circadian clock: period determination in the suprachiasmatic nuclei. Cell 91:855–860.

Loudon ASI, Wayne NL, Krieg R, Iranmanesh A, Veldhuis JD, Menaker M (1994) Ultradian endocrine rhythms are altered by a circadian mutation in the Syrian hamster. Endocrinology 135:712–718.

Marchant EG, Mistlberger RE (1996) Entrainment and phase shifting of circadian rhythms in mice by forced treadmill running. Physiol Behav 60:657–663.

Meijer JH, Rietveld WJ (1989) Neurophysiology of the suprachiasmatic circadian pacemaker in rodents. Physiol Rev 69:671–707.

Meijer JH, Schaap J, Watanabe K, Albus H (1997) Multiunit activity recordings in the suprachiasmatic nuclei: in vivo versus in vitro models. Brain Res 753:322–327.

Miller JD, Fuller CA (1992) Isoperiodic neuronal activity in suprachiasmatic nucleus of the rat. Am J Physiol 263:R51–R58.

Moore RY, Eichler VB (1972) Loss of a circadian adrenal corticosterone rhythm following suprachiasmatic nucleus lesions in the rat. Brain Res 42:201–206.

Morin LP, Goodless-Sanchez N, Smale L, Moore RY (1994) Projection of the suprachiasmatic nuclei, subparaventricular zone and retrochiasmatic area in the golden hamster. Neuroscience 61:391–410.

Mrosovsky N (1988) Phase response curves for social entrainment. J Comp Physiol [A] 162:35–46.

Murakami N, Takamure M, Takahashi K, Utunomiya K, Kuroda H, Etoh T (1991) Long-term cultured neurons from rat suprachiasmatic nucleus retain the capacity for circadian oscillation of vasopressin release. Brain Res 545:347–350.

Numan M, Numan M (1996) A lesion and neuroanatomical tract-tracing analysis of the role of the bed nucleus of the stria terminalis in retrieval behavior and other aspects of maternal responsiveness in rats. Dev Psychobiol 29:23–51.

Omata K, Kawamura H (1988) Effect of methamphetamine upon circadian rhythms in multiple unit activity inside and outside the suprachiasmatic nucleus in the golden hamster (*Mesocricetus auratus*). Neurosci Lett 95:218–222.

Prast H, Dietl H, Philippu A (1992) Pulsatile release of histamine in the hypothalamus of conscious rats. J Auton Nerv Syst 39:105–110.

Raitiere MN, Garyfallou VT, Urbanski HF (1995) Lesions in the bed nucleus of the stria terminalis, but not in the lateral septum, inhibit short-photoperiod-induced testicular regression in Syrian hamsters. Brain Res 705:159–167.

Ralph MR, Foster RG, Davis FC, Menaker M (1990) Transplanted suprachiasmatic nucleus determines circadian period. Science 247:975–978.

Reebs SG, Mrosovsky N (1989) Effects of induced wheel running on the circadian activity rhythms of Syrian hamsters: entrainment and phase response curve. J Biol Rhythms 4:39–48.

Rusak B, Zucker I (1979) Neural regulation of circadian rhythms. Physiol Rev 59:449–526.

Sawaki Y, Nihonmatsu I, Kawamura H (1984) Transplantation of the neonatal suprachiasmatic nuclei into rats with complete bilateral suprachiasmatic lesions. Neurosci Res 1:67–72.

Shibata S, Moore RY (1988) Electrical and metabolic activity of suprachiasmatic nucleus neurons in hamster hypothalamic slices. Brain Res 438:374–378.

Shinohara K, Honma S, Katsno Y, Abe H, Honma K (1995) Two distinct oscillators in the rat suprachiasmatic nucleus *in vitro*. Proc Natl Acad Sci USA 92:7396–7400.

Shioiri T, Takahashi K, Yamada N, Takahashi S (1990) Motor activity correlates negatively with free-running period, while positively with serotonin contents in SCN in free-running rats. Physiol Behav 49:779–786.

Silver R, LeSauter J, Tresco PA, Lehman MN (1996) A diffusible coupling signal from the transplanted suprachiasmatic nucleus controlling circadian locomotor rhythms. Nature 382:810–813.

Stephan FK, Zucker I (1972) Circadian rhythms in drinking behavior and locomotor activity of rats are eliminated by hypothalamic lesions. Proc Natl Acad Sci USA 69:1583–1586.

Thomson DJ (1982) Spectrum estimation and harmonic analysis. Proc IEEE 70:1055–1096.

Turek FW (1985) Circadian neural rhythms in mammals. Annu Rev Physiol 47:49–64.

van Reeth O, Losee-Olson S, Turek FW (1987) Phase shifts in the circadian activity rhythm induced by triazolam are not mediated by the eyes or the pineal gland in the hamster. Neurosci Lett 80:185–190.

Vautard R, Yiou P, Ghil M (1992) Singular-spectrum analysis: a toolkit for short, noisy chaotic signals. Physica D 58:95–126.

Vogelbaum MA, Menaker M (1992) Temporal chimeras produced by hypothalamic transplants. J Neurosci 12:3619–3627.

Watanabe K, Koibuchi N, Ohtake H, Yamaoka S (1993) Circadian rhythms of vasopressin release in primary cultures of rat suprachiasmatic nucleus. Brain Res 624:115–120.

Welsh DK, Logothetis DE, Meister M, Reppert SM (1995) Individual neurons dissociated from rat suprachiasmatic nucleus express independently phased circadian firing rhythms. Neuron 14:697–706.

Wichmann T, Vitek JL, DeLong MR (1995) Parkinson's disease and the basal ganglia: lessons from the laboratory and from neurosurgery. The Neuroscientist 1:236–244.

Wood RI, Newman SW (1993) Mating activates androgen receptor-containing neurons in chemosensory pathways of the male Syrian hamster brain. Brain Res 614:65–77.

Yamada N, Shimoda K, Ohi K, Takahashi S, Takahashi K (1988) Free-access to a running wheel shortens the period of free-running rhythm in blinded rats. Physiol Behav 42:87–91.

Yamada N, Shimoda K, Takahashi K, Takahashi S (1990) Relationship between free-running period and motor activity in blinded rats. Brain Res Bull 25:115–119.

Yamazaki S, Ishida Y, Inouye S-IT (1994) Circadian rhythms of adenosine triphosphate contents in the suprachiasmatic nucleus, anterior hypothalamic area and caudate putamen of the rat: negative correlation with electrical activity. Brain Res 664:237–240.

Yamazaki S, Alones VE, Block GD, Menaker M (1997) Functional connection between the circadian and motor systems. Soc Neurosci Abstr 23:790.